Supplementary Materials: Study on the self-repairing effect of nanoclay in powder coatings for corrosion protection

Marshall Shuai Yang [1,2], Jinbao Huang [1,3], Hui Zhang [1,*], James Joseph Noël [2,4,*], Yolanda Susanne Hedberg [2,4,*], Jian Chen [2], Ubong Eduok [2], Ivan Barker [4], Jeffrey Daniel Henderson [4], Chengqian Xian [5], Haiping Zhang [6] and Jesse Zhu [1]

[1] Department of Chemical and Biochemical Engineering, Western University, London, ON N6A 5B9, Canada; marshall.yang@uwo.ca (M.S.Y.); jhuan467@uwo.ca (J.H.); jzhu@uwo.ca (J.Z.)
[2] Department of Chemistry, Western University, London, ON N6A 5B7, Canada; jchen496@uwo.ca (J.C.); ueduok@uwo.ca (U.E.)
[3] Zhengzhou Research Institute, Harbin Institute of Technology, Zhengzhou 450000, China; jinbao.huang@hit.edu.cn
[4] Surface Science Western, Western University, London, ON N6G 0J3, Canada; ivan.barker@uwo.ca (I.B.); jhende64@uwo.ca (J.D.H.)
[5] Department of Statistical and Actuarial Sciences, Western University, London, ON N6A 5B7, Canada; cxian3@uwo.ca
[6] Collaborative Innovation Center of Chemical Science and Engineering (Tianjin), School of Chemical Engineering and Technology, Tianjin University, Tianjin 300072, China; hpzhang@tju.edu.cn
* Correspondence: hzhang1@uwo.ca (H.Z.); jjnoel@uwo.ca (J.J.N.); yhedberg@uwo.ca (Y.S.H.); Tel.: +1-519-661-2111 (ext. 81294) (H.Z.); +1-519-661-2111 (ext. 88029) (J.J.N.); +1-519-661-2111 (ext. 86248) (Y.S.H.)

1. Electrochemical measurement results

The total impedance of the EEC (equivalent electrical circuit) for data fitting in Figures 9e and 13e is expressed as Equation. S1:

$$Z_{total} = R_s + \frac{1}{Q_{coat}(j\omega)^{\alpha_{coat}} + \frac{1}{R_{pore} + \frac{1}{Q_{dl}(j\omega)^{\alpha_{dl}} + \frac{1}{R_{ct} + Z_{W_s}}}}} \quad \text{(S1)}$$

2. Breakpoint frequency analysis

For all the EIS measurements, only the lower breakpoint frequencies (f_l) were available, and these values are plotted for the coatings prepared from both formulae C1–04%-PC and C2–08%-PC in Figure S1c. In line with the R_p values, the coatings with larger particles at their optimal dosage exhibited a better barrier effect, as indicated by the lower f_l values over time. The breakpoint frequency analysis indicated abrupt changes in the coating behavior on Days 7 (C1–04%-PC) and 3 (C2–08%-PC), which were close to the findings of Days 9 and 4 in the Nyquist plots and subsequent EIS fitting. These changes confirmed the inception of localized steel corrosion, after which These changes confirmed the initiation of localized corrosion of the steel, after which the diffusion of soluble corrosion products became important, as indicated by the need for a Warburg element in the EIS equivalent circuit.

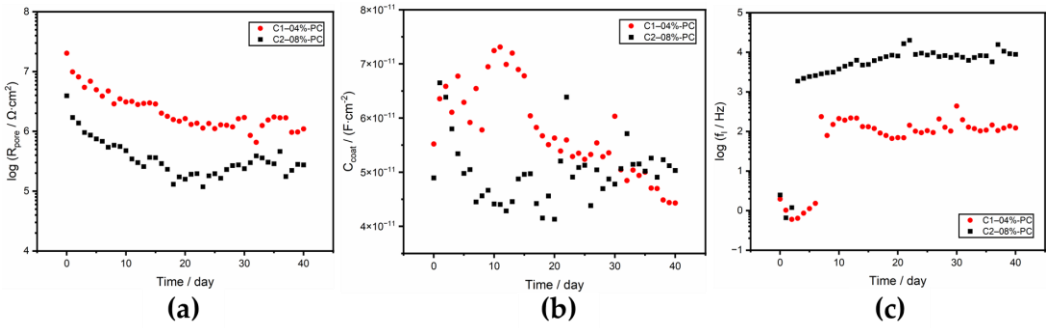

Figure S1. Fitted values of (a) R_{pore}, (b) C_{coat}, and (c) lower breakpoint frequencies determined on coatings prepared from the formulae C1–04%-PC and C2–08%-PC.

3. Corrosion products and corrosion reactions

X-ray diffraction (XRD) and Raman spectroscopy were used to identify the corrosion products and reactions in the coatings. The characteristic peaks for individual species were labeled on the diffraction patterns and spectra in Figure S2a–d.

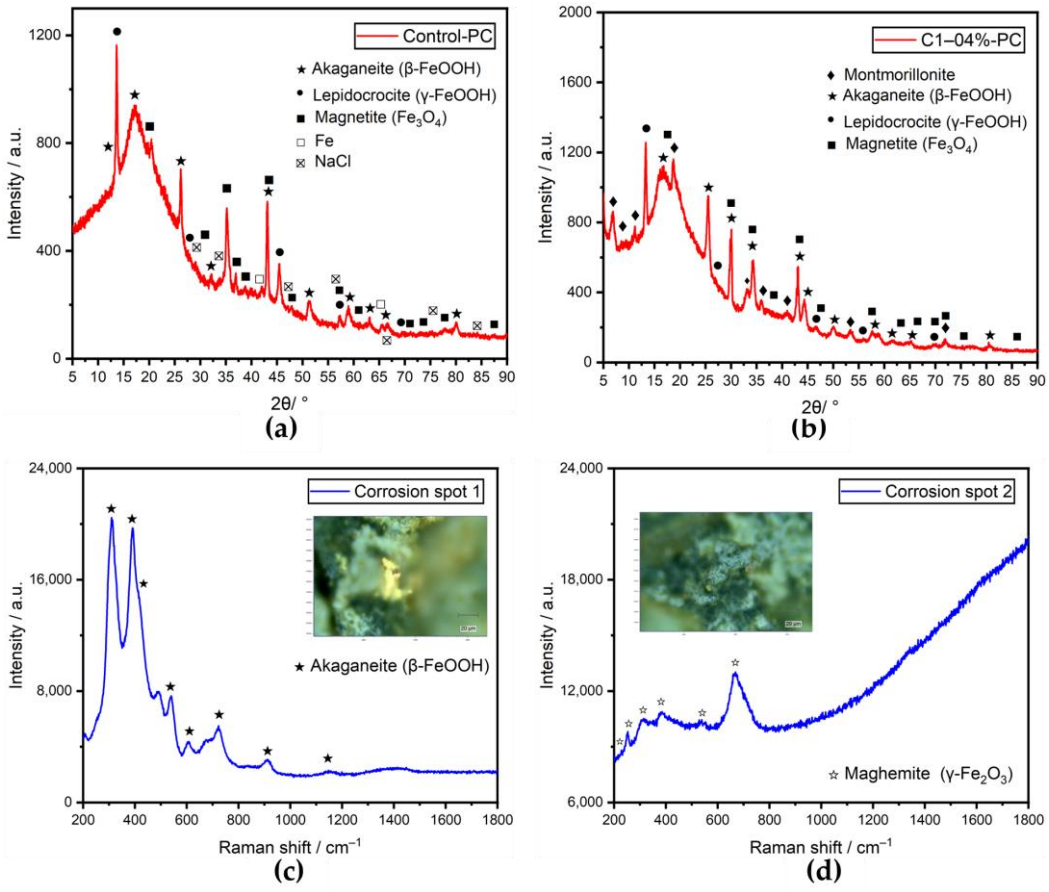

Figure S2. (a,b) XRD patterns and (c,d) Raman spectra of the coatings prepared from the formulae PC-Control and C1–04%-PC.

Akageneite (β-FeOOH), lepidocrocite (γ-FeOOH), magnetite (Fe_3O_4), and maghemite (γ-Fe_2O_3) were detected as corrosion products, with the presence of Cl^- facilitating the formation of akageneite [74].

The corrosion reaction of the steel substrate under the coating films was determined to involve the oxidation of Fe to $Fe(OH)_2$, followed by the oxidation of $Fe(OH)_2$ through multiple routes (Equation S2. 9, Figure S3), with the coatings functioning as barrier layers.

The presence of nanoclay particles in the coatings did not affect the corrosion reaction or the species formed [74].

$$\begin{gathered} Fe \rightarrow Fe^{2+} + 2e^{-} \text{ (anodic)} \\ 2H_2O + O_2 + 4e^{-} \rightarrow 4OH^{-} \text{(cathodic)} \\ 2Fe + O_2 + 2H_2O \rightarrow 2Fe(OH)_2 \end{gathered} \quad \text{(S2)}$$

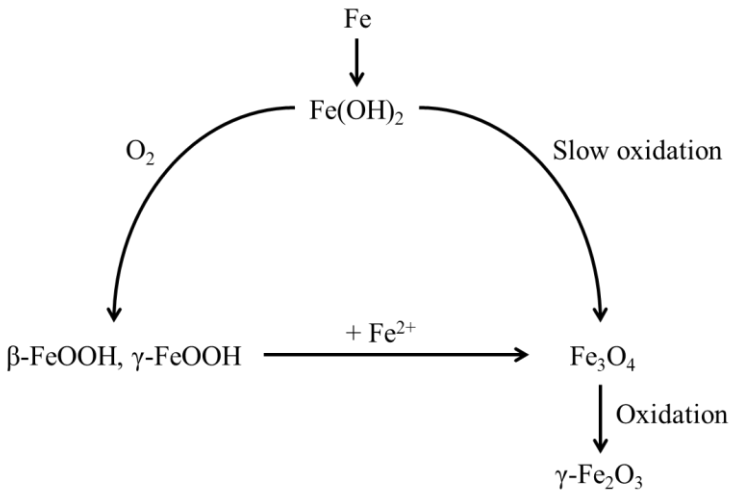

Figure S3. Corrosion reactions of the steel substrate under the coating films.

This study has employed long-term electrochemical (in an electrolyte) and salt spray (in atmosphere) testing approaches and found slightly contradicting results because of the nanoclay swelling, which in some cases had a self-healing effect, required water from the electrolyte. This finding might imply that the self-healing effect of nanoclay-containing coatings might depend on the humidity and environmental conditions during service life. Future studies should investigate the effects of these factors.